EUROFUSION WPJET1-CP(16) 15144

S Wiesen et al.

Impact of the JET ITER-like wall on H-mode plasma fuelling

Preprint of Paper to be submitted for publication in
Proceedings of 26th IAEA Fusion Energy Conference

This work has been carried out within the framework of the EUROfusion Consortium and has received funding from the Euratom research and training programme 2014-2018 under grant agreement No 633053. The views and opinions expressed herein do not necessarily reflect those of the European Commission.

Impact of the JET ITER-like wall on H-mode plasma fueling

S. Wiesen[1], S. Brezinsek[1], M.Wischmeier[2], E. De la Luna[3], M.Groth[4], A. E. Jaervinen[5], E. de la Cal[3], U. Losada[3], A. M. de Aguilera[3], L. Frassinetti[6], Y. Gao[1,7], C. Guillemaut[8], D.Harting[9], A. Meigs[9], K. Schmid[2], G. Sergienko[1] and JET contributors[*]

EUROfusion Consortium, JET, Culham Science Centre, Abingdon, OX14 3DB, UK
[1]Forschungszentrum Jülich GmbH, Institut für Energie- und Klimaforschung – Plasmaphysik, Partner of the Trilateral Euregio Cluster (TEC), 52425 Jülich, Germany
[2]Max-Planck-Institut für Plasmaphysik, 85748 Garching bei München, Germany
[3]Laboratorio Nacional de Fusion, CIEMAT, 28040, Madrid, Spain
[4]Aalto University, Association EURATOM/Tekes, Otakaari 4, Espoo, Finland
[5]Lawrence Livermore National Laboratory, Livermore, CA 94550, USA
[6]Association VR, Fusion Plasma Physics, KTH, SE-10044 Stockholm, Sweden
[7]Institute of Plasma Physics, Chinese Academy of Sciences, Hefei 230031, China
[8]Instituto de Plasmas e Fusão Nuclear, IST, Univ. de Lisboa, P-1049-001, Lisboa, Portugal
[9]CCFE, Culham Science Centre, Abingdon OX14 3DB, UK
[*]see the author list of "Overview of the JET results in support to ITER" by X. Litaudon et al. to be published in Nuclear Fusion Special issue: overview and summary reports from the 26th Fusion Energy Conference (Kyoto, Japan, 17-22 October 2016)

E-mail contact of main author: s.wiesen@fz-juelich.de

Abstract. JET ITER-like wall (ILW) experiments show that the edge density evolution is strongly linked with the poloidal distribution of the ionization source. The fueling profile is more delocalized as compared to JET-C (JET with carbon-based plasma-facing components PFCs). Compared to JET-C the H-mode pedestal fueling cycle is dynamically influenced by a combination plasma-wall interaction features, in particular: 1) Edge-localized modes (ELMs) induced energetic particles are kinetically reflected on W divertor PFCs leading to distributed refueling away from the divertor depending on the divertor plasma configuration, 2) delayed molecular re-emission and outgassing of particles being trapped in W PFCs (bulk-W at the high field side and W-coated CFCs at the low field side) with different fuel content and 3) outgassing from Be co-deposits located on top of the high-field side baffle region shortly after the ELM. Dedicated JET-ILW H-mode experiments have been executed to disentangle aforementioned effects. A direct measurement of the particle flows in the SOL is not possible in JET and the spatial and temporal evolution of the poloidal fueling profile can only be derived from 2D edge plasma simulations.

1. Introduction

The JET ILW consists of a beryllium first-wall and tungsten armor in the divertor [1] and has demonstrated to perform very successfully for plasma-wall interaction (PWI) and plasma operation with the plasma-facing material selection foreseen in ITER [2]. The JET-ILW demonstrated the low expected long-term fuel retention in the metallic environment (factor 10-15 less than JET-C) predominantly due to co-deposition in Be and about 1/3 due to implantation and surface coverage in Be and W [3,4] as well as allows fast isotope exchange of the accessible reservoir in the PFCs which is about 1/10 of the one in JET-C [5,6]. Stiff transport determines the evolution of the central density in a tokamak plasma and is thus mainly driven by the edge pedestal height if not otherwise fueled by pellet ablation. Initial comparisons of JET-ILW with JET-C (JET with PFCs made of carbon-fiber composites) showed that the evolution of the edge

density is strongly linked with the level of recycling [7] as with increasing density a delay is observed before the pedestal density recovers after an ELM-crash. As a consequence a degraded confinement $H_{98,y} < 1.0$ is generally observed in high current unseeded baseline scenarios as an increased density enforced by deuterium fueling is required to avoid tungsten accumulation. To mitigate the reduced confinement divertor plasma configurations with the strike-lines close to the divertor corners are preferred as pumping is enhanced [8] and direct reflection of sputtered W into the confined region inhibited.

The pre-ELM pedestal width Δn_{ped} and height n_{ped} is significantly influenced by the poloidal and radial ionization profile just inside the separatrix. Regression analysis of JET-ILW H-mode pedestal profiles revealed recently that Δn_{ped} depends on pedestal collisionality ν^*_{ped} [9]. Indeed, the number of deuterium ionized close to the separatrix depends directly on the global particle flux balance within the scrape-off layer (SOL) and is a function of neutral and plasma transport as well as PWI. During JET-C operation, the recycled deuterium flux in the divertor typically dominated the externally applied gas flux and the neutrals cross dominantly the X-point region to refuel the plasma core. The strong localized fueling process of the core plasma allowed reliable predictions of the pedestal performance by using edge stability models like EPED [10]. With the installation of the JET-ILW it has become evident that this simplistic picture is insufficient as the poloidal distribution of the ionization source and the fueling profile have become more delocalized and the ratio of recycling to injected deuterium for fueling changed with respect to JET-C with increasing importance of fueling by injection and localized recycling dynamics.

The impact of the metallic wall on the fueling process has been recovered very early during the first JET-ILW campaigns. For example from L-mode discharges in low-recycling conditions [11] one can estimate that the ratio of injected particles Γ_{inj} to the total recycling flux Γ_{rec} is of order 3-5 higher in JET-ILW than in JET-C (with Γ_{rec} being derived from D_α radiation photon emission fluxes converted into a recycling flux using integral S/XB values [12]). In H-mode this ratio can be even larger as energetic particles can enter the deeper into the metallic bulk-W/W-coated CFC surface layers in the divertor so that for achieving a given pedestal density n_{ped} a throughput of one order of magnitude higher is required in JET-ILW as without carbon the additional D particle source due to chemical erosion of thick a-C:D layers with high fuel content (C:D in the average of 0.5) is effectively switched off (compared to a similar JET-C discharge 15 times less residual C is abundant in JET-ILW).

With the JET-ILW it is observed that the H-mode fueling cycle dynamics during and between ELMs is impacted by the evolution of the global particle balance. In particular, the poloidal fueling profile is dynamically influenced by the following PWI effects:

1. ELM induced energetic particles with up to 4-5 times equivalent to pedestal temperature [13] are kinetically reflected on metallic W divertor PFCs leading to a more distributed refueling away from the divertor. For example, the particle reflection coefficient for a D-particle with 1 keV impact energy increases from 0.1 to 0.5 when moving from C to W and likewise, the energy reflection coefficient increases by one order of magnitude [14]. This induces the kinetic-geometric effect of reflected particles amending the poloidal ionization source profile (cf. Fig. 1). Depending on the divertor plasma shape (e.g. horizontal vs. vertical target or corner configuration) recycled neutral molecules and atoms reach the private or common flux zone where they are dissociated and ionized, or, pumped away as particles may or may not reach the pump ducts more easily.
2. Molecular re-emission can be delayed as particles can be trapped in W PFCs, bulk-W and W-coated CFCs with different fuel content, resulting in retarded recycling after the

ELM due to surface temperature T_{surf} dependent outgassing effects and heat diffusion into near surface layer (μm) [15].

3. At the main-chamber wall Be is eroded and material migration leads to deposition of Be predominantly on the upper inner target plate [16]. Re-erosion and multistep transport along the target plate as in JET-C doesn't take place due to absence of chemical erosion at low impact energy [17]. Very recently it was found at JET that during the ELM outgassing does occur from these deposition areas leading to a localized fueling effect on the high-field side (HFS).
4. Nitrogen seeding (or hydrocarbons C_xD_y) may lead to the formation of surface chemical compounds which can store temporarily D particles in the wall and other chemical transport channels come into play (e.g. due to formation of ammonia or carbon co-deposits at the wall).

In this paper we focus on point 2 and 3. The impact of kinetic effects on recycling and W sputtering has been dealt with by other authors already [13, 18] as well as the impact of the selection of the divertor configuration [8,19]. Generally the neutral kinetics effects are already included being an essential part of the fluid-kinetic edge transport codes like SOLPS-ITER [20] or EDGE2D-EIRENE. The impact of nitrogen on confinement is being dealt with in a separate contribution [21].

2. Setup of experiment

In this paper we present results from dedicated JET-ILW H-mode experiments during the C30C campaign in 2012 [3] with I_p/B_t = 2.0MA/2.4T, low-triangularity, auxiliary neutral beam injection P_{NBI}=11MW in semi-horizontal divertor configurations with typical thermal energy drops of 160kJ per ELM. The experiments focused on the "footprint in material migration and retention" and assessment of recycling behavior as well as outgassing effects. The ELMs appeared in 6 seconds long flat-top phases of the discharges with frequency of about 30 Hz. The gas injection rate was in the order of $1.0x10^{22}$ Ds^{-1} into the divertor feed-forward with active cryo-pumps. The magnetic configuration in the plasma series (accumulated 900s in H-mode) on semi-horizontal configuration, i.e. the ISP on vertical target (tile 3), W-coated CFC) and OSP on the bulk-W divertor target plate (tile 5). The strike lines were static and positioned to identify well defined surface temperatures T_{surf} measured by the JET divertor IR system [22].

Fig. 2 depicts coherently averaged outer-midplane n_e and T_e profiles for the time just before an ELM-crash (0ms), shortly after the ELM with maximum drop in pedestal pressure (1.2ms) and during the ELM recovery (5.6ms) at which point the n_e profile has just reached its minimum and starts to recover. At that time T_e has already started to increase which is mainly driven by the power entering the pedestal from the plasma core. Such a delayed recovery of the density after the ELM was not observed in JET-C with much shorter ELM cycles.

The recycling flux close to the divertor target plates was measured by Langmuir probes as well as spectroscopically by D_α and molecular emission. A spectroscopic camera was used to discriminate the D_α and WI emission on the HFS top and bottom divertor during the ELM and in the inter-ELM period [23] (c.f. Fig 3).

3. Fast outgassing from bulk-W/W-coated CFC and impact on plasma H-mode fueling

The impact of retention, desorption and recycling during the ELM on the divertor conditions has been addressed in [15] for the same set of C30C discharges. ELM-induced desorption from saturated near-surface layers and implantation W regions as well as deep ELM-induced

deuterium implantation under varying baseline temperature conditions at the bulk-W tile takes place as during the discharge T_{surf} rises from a base level of about 160 °C exceeding up to 1400 °C at the end of the flat-top phase close to the OSP. The temporal and spatial evolution of T_{surf} of a set of coherently averaged ELM bursts is depicted in Fig. 4. About 1600 individual ELM footprints taken from the last 2.0s of the flat-top phase during the discharges with T_{surf}>800 °C where the temporal ELM footprint evolution appears self-similar. Also shown in Fig. 4 are the coherently averaged evolutions of the heat-flux density profiles measured by the IR system as well as the saturation current profiles along the horizontal target plate. The initial particle flux peak occurs almost at the same time with the ELM driven heat flux arriving at the plate. The slower convective nature of particle transport compared to the fast heat conduction is likely responsible for a slight delay of about 1ms. One can clearly identify a second pronounced peak in the J_{sat} signal about Δt~8ms after the first particle flux peak which has not been observed in JET-C. Typically in JET-ILW, this secondary peak has no correspondence to the impinging Be ion flux and the W sputtering influx as seen from Fig. 5 for a different but similar JET-ILW type-I ELMy H-mode discharge which indicates that the secondary peak is not related to ions from the pedestal region as it occurs already well within the slow recovery phase of the pedestal. Also the impact energy must be low as no W sputtering by Be or D occurs at the point of the second peak (W sputter threshold at 60eV for Be ions and 300eV for D ions [2]). The coherent appearance of both impinging ions (J_{sat}) and D_α radiation suggests that the origin of the second peak is related to a temporary appearance of localized recycling (low energy) at the target plate.

The aforementioned observations are based on data gathered from the last 2.0s part of the flat-top phase of C30C discharges only. In this phase T_{surf} has saturated in the region 1200 °C -1400 °C. However, the ELM signature has already been found to be strongly dependent on T_{surf} [15]. Specifically, the peak W surface temperature exhibits a qualitative change in the temporal signature (cf. fig. 3 in [15]). At the lowest accessible surface temperatures (T_{surf} = 300 °C < 450 °C) the ELM footprints show the shortest ELM duration and the signatures look clean, similar to the ELMs found in JET-C. However, at surfaces temperatures above a given threshold T_{surf} > 500 °C the ELM signatures become different. In the beginning of the ELM the typical temperature rise of about 100 °C when the heat load arrives at the plate, but afterwards a pronounced drop in temperature after the end of the ELM crash is observed. This drop is caused by local plasma cooling due to enhanced D_2 desorption at T_{surf} > 500 °C at the bulk-W PFC which reduces the inter-ELM heat load reaching the plate before the next ELM occurs. The outgassing, which is governed by diffusion of particles out of the W PFC surface, is quite localized in radial direction and depends on the fuel content in the W surface layers as well as T_{surf}. By increasing T_{surf} even further (the PFCs are inertially cooled) the desorption of D_2 is reduced again as less D particles can be stored in the W surface.

Currently, there is further statistical analysis ongoing to discriminate the duration between the first and the second peak in J_{sat} during an ELM burst, as well as the height of the secondary particle flux peak to understand and see whether there is any correlation of delay time Δt or height Δh of the secondary recycling peak and of the local surface temperature T_{surf}.

Model wise, the process of outgassing can be described by trap-diffusive models as described in for example in [24]. These models must make assumptions about the impinging heat and particle flux as well as about the concentration of trap locations in the W or Be material solute. With the coherently averaged transients for particle and heat flux footprints of C30C discharges, the derived recycling coefficient during the ELM R^{ELM} can of order unity [24]. With increasing trap-concentration in the W-solute the calculated ratio ξ=effusing/implanted flux may vary between 0.4-2.0 depending on the assumption of the trap-concentration in the W solute [25] and subsequently, one derives by assuming a particle reflection coefficient of ~0.5 for 1keV D-particles on W-PFC [14] and for the ξ~0.5 an effective recycling coefficient R_{ELM} ~ 0.75.

The JINTRAC integrated code [26] (a self-consistent approach of the coupled 1D core/pedestal transport code JETTO and the 2D edge plasma/PWI code EDGE2D-EIRENE) has been employed to assess the impact of recycling conditions for the C30C type-I ELM discharges [27]. For this analysis a new but very simple dual-reservoir model has been introduced into the code (one reservoir for each HFS/LFS target plate of size of the order 10^{20} particles). In the short time between reservoir emptying (after an individual ELM-burst arrived at the target plate) and replenishing the reservoir by the impinging target particle flux, the recycling coefficient R^{ELM} has been reduced to values between 0.3 and 0.5. Outside this short phase lasting a couple of ms (depending on the reservoir size) the recycling coefficient has been set to unity. With this model setup (oversimplified as it ignores the T_{surf} dependency on R^{ELM} and reservoir size) the model does show a delayed recovery of the pedestal density of the order of 10ms. However the model does not recover the slow response of T_{ped} on the ELM as reported in [7,28]. It is very likely that other effects like a change in MHD stability after the ELM (as response to changes for example in separatrix or fueling conditions) do play an important role in the recovery of T_{ped}. It should be noted that the pedestal transport model in JINTRAC does not include a coupling of density and temperature as for example demanded by [29] and other authors.

4. Outgassing from Be co-deposits during ELM at the high-field side (HFS)

In the JET-ILW the major fraction of eroded Be particles from the main-chamber are co-deposited near or on top the HFS baffle region [16] (c.f. Fig.1, tile 1). These co-deposits can store a large fraction of D particles (on average: D:Be atomic ratio about 10%, some higher ratio up to 40% directly at the surface [30]). Recently, in the JET-ILW C35-C36 campaigns in 2015 similar plasmas to the ones in C30C have been executed (I_p/B_t=2.0MA/2.4T, P_{NBI}=12MW, low-triangular semi-horizontal configuration with OSP on tile 5, the ISP located high or low on vertical tile 3) in which significant D_α emission has been observed on top of the HFS tile 1 after the ELM due to surface heating using a fast acquisition camera system [31] with a sampling rate of up to 70kHz capable in discriminating the areas emissions in the divertor (c.f. Fig. 6). At the ELM the D_α emission increases near the bottom of the HFS divertor but is then followed shortly after (1ms after) by a long lasting and strong secondary D_α emission peak obviously stemming from D particles being outgassed from the Be co-deposits on HFS tile 1. The localized recycling in this area decays on a time-scale of about 6ms or more and must add up as an additional D particle fueling influx due to its vicinity to the separatrix near and above the X-point. Further analysis of this localized recycling process which is seemingly dependent on local conditions (local fluxes, surface conditions, position of strike points) is still ongoing.

5. Conclusions

In contrast to JET-C, metallic devices as the JET-ILW exhibit a complex picture of the recycling process in ELMy H-mode discharges. Outgassing by surface temperature dependent desorption of particles near the strike-points on the bulk-W/W-coated CFC PFCs as well as from Be co-deposits in localized areas do lead to an inhomogeneous poloidal fueling profile evolving in time. Depending on the local conditions the number of recycled particles change locally. At the moment it seems difficult to disentangle for example the occurrence of a secondary recycling flux peak occurring a few ms after the ELM burst as several processes happen at the same time on overlapping time-scales (outgassing from bulk-W/W-coated CFC as well as from Be co-deposits on top of the HFS baffle). Unfortunately, a direct and time-dependent measurement of the plasma and neutral flows in the SOL is not possible in JET. The full data set should be taken to derive numerically the poloidal ionization and fueling profiles by using for example the SOLPS-ITER code package [20] to compare the H-mode fueling efficiency between JET-ILW

and JET-C. By the time of writing the simulation attempts to take into account for example the extra fueling source like the additional HFS recycling shortly after the ELM from outgassing of Be co-deposits are still ongoing. In the near future the SOLPS-ITER is extended towards the inclusion of most of the aforementioned effects. Foreseen new features include a) revised recycling models going beyond oversimplified reservoir models (e.g. [27]), i.e. a coupling to trap-diffusive models [24] into the EIRENE neutrals code monitoring also the evolution of surface temperatures in time for the bulk-W/W-coated CFC divertor tiles as well as for main-chamber Be PFCs and co-deposited areas, b) extension of the plasma grid up to the first wall to improve model for global Be-erosion and migration, and c) as for the JINTRAC model, a coupling to a core/pedestal code also for SOLPS-ITER simulations.

Acknowledgements

This work has been carried out within the framework of the EUROfusion Consortium and has received funding from the Euratom research and training programme 2014-2018 under grant agreement No 633053. The views and opinions expressed herein do not necessarily reflect those of the European Commission.

References

[1] G. F. Matthews et al., Phys. Scripta T145 (2011) 014001
[2] S. Brezinsek et al., J. Nucl. Mater. 463 (2015) 11-21
[3] S. Brezinsek et al., Nucl. Fusion 53 (2013) 083023
[4] V. Philipps et al., J. Nucl. Mater. 438 (2013) S1067
[5] T. Loarer et al., J. Nucl. Mater. 463 (2015) 1117
[6] T. Wauters et al., J. Nucl. Mater. 463 (2015) 1104
[7] E. De la Luna et al., IAEA FEC 2014
[8] E. Joffrin et al, IAEA FEC 2014
[9] L Frassinetti et al., subm. Nucl Fusion 2016
[10] P.B. Snyder et al., Nucl. Fusion 51 (2011) 103016
[11] M. Groth et al., Nucl. Fusion 53 (2013) 093016
[12] S. Brezinsek et al., Plasma Phys. Control. Fusion 47 (2005) 615
[13] C. Guillemaut et al., Phys. Scr. T167 (2016) 014005
[14] W. Eckstein et al., Report IPP 9/132 (2002)
[15] S. Brezinsek et al., Phys. Scr. T167 (2016) 014076
[16] M. Mayer et al., Phys. Scr. T167 (2016) 014051
[17] S. Brezinsek et al., Nucl. Fusion 55 (2015) 063021
[18] I. Borodkina et al., PSI 2016, subm. to NME 2016
[19] P. Tamain et al., J. Nuc. Mater. 463 (2015) 450
[20] S. Wiesen et al., J. Nucl. Mater. 415 (2011) S535
[21] C. Giroud et al., this conference
[22] I. Balboa et al., Rev. Sci. Instrum. 83 (2012) 10D530
[23] A. Huber et al., Fusion Eng. and Des. 88 (2013) 1361
[24] K. Schmid et al., Phys. Scr. T167 (2016) 014025
[25] K. Schmid, priv. communication
[26] M. Romanelli et al., Plasma and Fusion Research, Vol. 9 (2014) 3403023
[27] S. Wiesen et al., Contrib. Plasma Phys. 56, No. 6-8 (2016) 754
[28] E. de la Luna et al., this conferemce
[29] B. Scott et al., Contrib. Plasma Phys. 56, No. 6-8 (2016) 534
[30] K. Heinola et al., this conference
[31] E. de la Cal et al., Proc. 39th EPS Conf. on Plasma Physics (Stockholm, Sweden, 2012)

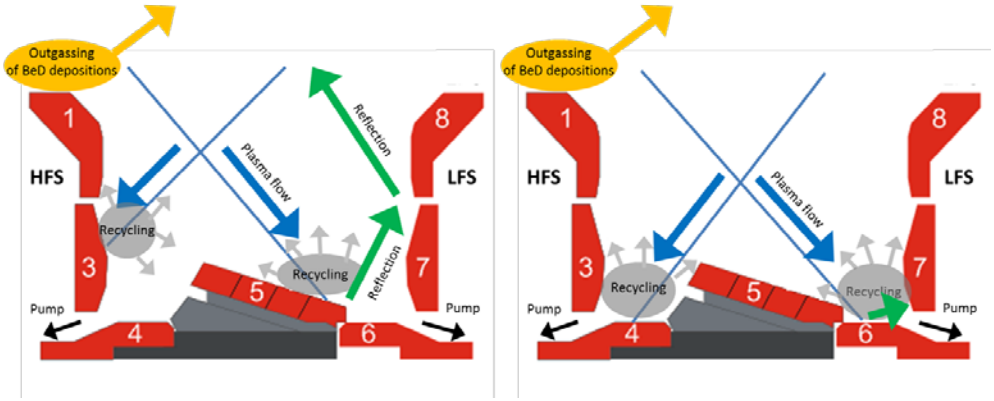

FIG. 1. Schematic view of particle recycling during the ELM leading to a delocalised poloidal fuelling profile. Left: semi-horizontal configuration, Right: corner configuration

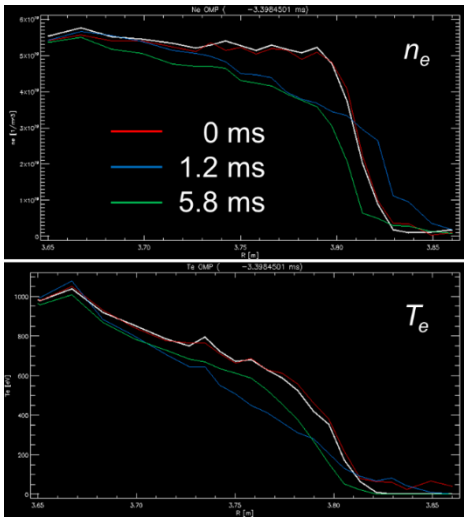

FIG. 2. Coherently averaged high-resolution Thomson Scattering profiles of pedestal density and temperature just before the ELM (0ms), at the drop with maximum drop in pedestal pressure (1.2ms) and during the recovery phase of the pressure (5.8ms). The averaging procedure assumed that the point in time of the ELM-crash can be identified with the BeII signal measured from vis. spectroscopy of at the inner wall (not shown).

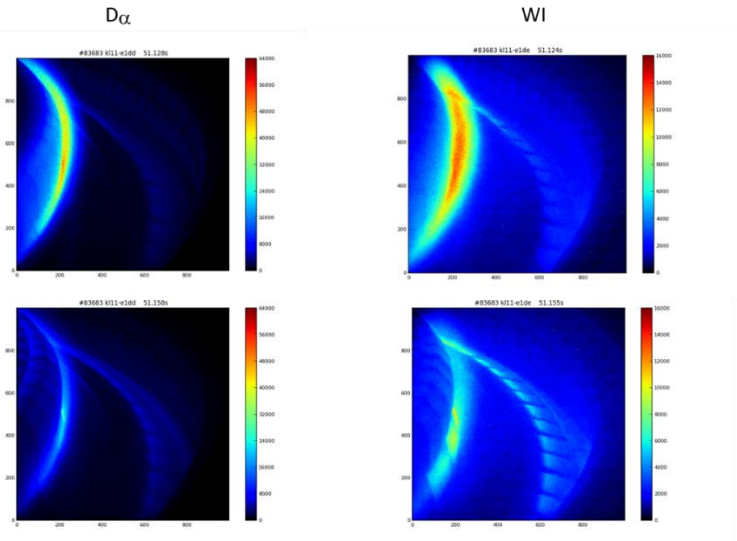

FIG. 3. Fast acquisition camera data to discriminate the Dα emission (left) on the HFS top and bottom divertor during the ELM (top) and in the inter-ELM period (bottom). Right: Identical views of the same camera system displaying WI emission during (top) and after (bottom) the ELM.

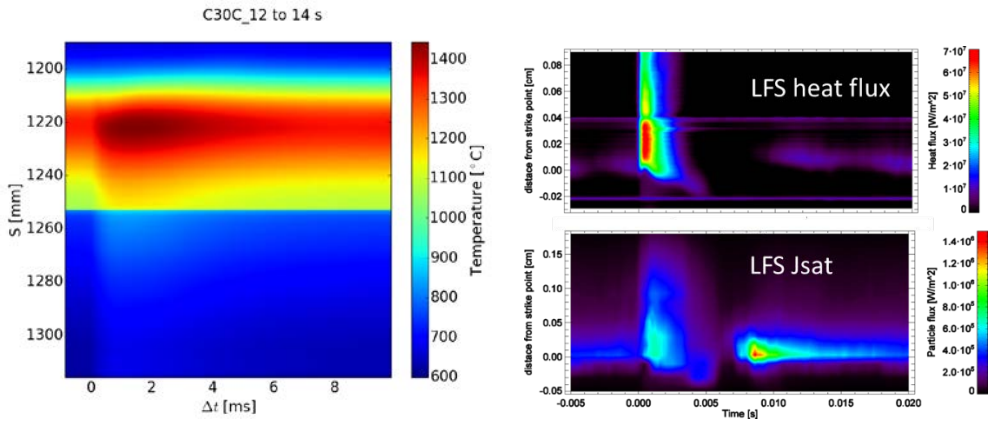

FIG. 4. Evolution of a typical type-I ELM event of the C30C campaign including the pre/post phase of the ELM (shown are coherently averaged LFS profiles over many ELMs of identical discharges). Left: T_{surf} evolution derived from IR thermography (S is the coordinate along the plate), Right: corresponding heat flux arriving at the outer target plate and evolving saturation current J_{sat}.

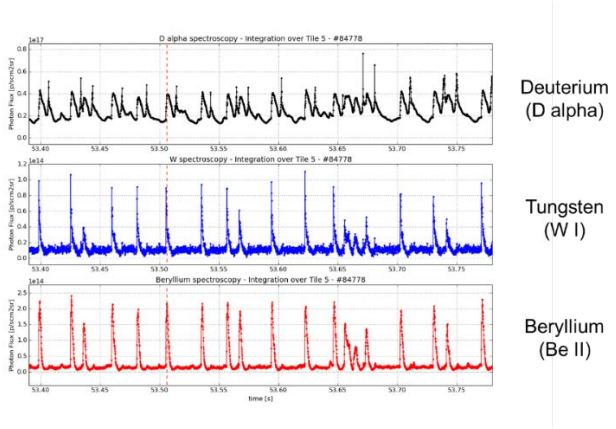

FIG. 5. From top to bottom: time-traces of emissions from Dα, WI and BeII (JPN #84778)

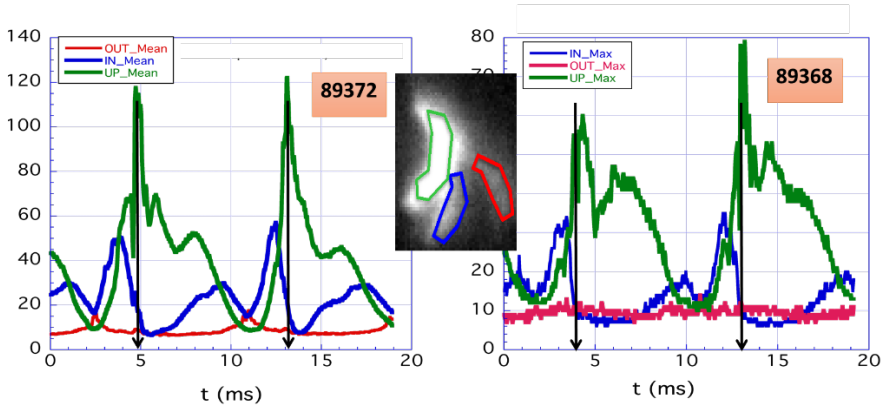

FIG. 6. Fast camera signals (arb. units) disentangling Dα emission from outer divertor (red), inner divertor (blue) and on top of HFS tile 1 (green)